X-693-70-209
PREPRINT

NASA TM X- 63952

TYPE III SOLAR RADIO BURST STORMS OBSERVED AT LOW FREQUENCIES

PART II: AVERAGE EXCITER SPEED

JOSEPH FAINBERG
R. G. STONE

JUNE 1970

GSFC
GODDARD SPACE FLIGHT CENTER
GREENBELT, MARYLAND

TYPE III SOLAR RADIO BURST STORMS OBSERVED AT LOW FREQUENCIES
PART II: AVERAGE EXCITER SPEED

by

Joseph Fainberg and R.G. Stone
Radio Astronomy Branch
Laboratory for Extraterrestrial Physics
Goddard Space Flight Center
Greenbelt, Maryland

ABSTRACT

Storms of type III solar radio bursts observed from 5.4 to 0.2 MHz consist of a quasi-continuous production of type III events observable for a half solar rotation but persisting in some cases for well over a complete rotation (Fainberg and Stone, 1970). The observed burst drift rates are a function of the heliographic longitude of the associated active region. This apparent drift rate dependence is a consequence of the radio emission propagation time from source to observer. Based on this dependence, a least squares analysis of 2500 drift rates between frequencies in the 2.8 to 0.7 MHz range yields an average exciter speed of 0.38c for the height range from approximately 11 to 30 $R_\odot$. In conjunction with the available determinations of exciter speeds of 0.33c close to the sun, i.e. less than 3 $R_\odot$, and with in situ measurements of 40 keV solar electrons by space probes, the present results suggest that the exciters are electron packets which propagate with little deceleration over distances of at least 1 A.U.

I. INTRODUCTION

According to the plasma hypothesis (Wild, 1950) the frequency drift of type III solar radio bursts is produced by the outward motion of a disturbance, the exciter, which generates plasma waves of decreasing frequency as the exciter travels through the corona along a path of decreasing electron density. It is also believed that the exciter is a packet of superthermal electrons. There are a number of general reviews of solar radio emission (Wild et al., 1963; Takakura, 1967) which include a discussion of the type III emission mechanism and the present state of the theory. The first direct confirmation of the plasma hypothesis was provided by the swept frequency interferometric observations of Wild et al.(1959) at frequencies of 45 and 60 MHz. These observations yielded exciter speeds in the range from 0.2 to 0.8 times that of light with an average value of about 0.45c. More recent directional observations in the same frequency range give similar results (e.g. Kundu et al., 1970). The plasma origin for type III bursts is generally accepted although many aspects of the process are not fully understood. On occasion alternate mechanisms are suggested (Slysh, 1967; Kuckes and Sudan, 1969).

In the remainder of this paper, we assume that the type III bursts are preferentially observed when the exciters travel

along active region streamers. Such streamers have an average electron density enhanced relative to the solar wind so that the radio emission is able to escape over a wider angular range than for a spherically symmetric corona.

In the absence of direct observations of the source position, an alternate method of determining the exciter speed requires the use of a model for the electron density gradient along the path of the disturbance. In this case the frequency drift obtained from dynamic spectra can be used to obtain the exciter speed, assuming radial motion of the disturbance. This approach has been used extensively over various parts of the spectrum above 6 MHz (Wild, 1950; Wild et al., 1954; Malville, 1962; Elgaroy and Rodberg, 1963; Hughes and Harkness, 1963; Stewart, 1965).

A weakness in this approach is the necessity for assuming an electron density model along the path traversed by the disturbance. Distributions such as 10 times the Baumbach-Allen model (Allen, 1947) as well as that proposed by Newkirk (1961) for active regions have been used. The latter model appears to give reasonable values at least to a few solar radii. Beyond 5-10 $R_{\odot}$, however, where direct observations of the K-corona do not provide electron densities, the choice of a model is far more difficult. Alternately, if the exciter speed were known, dynamic spectra could provide the electron density gradient

along the exciter path.

Malville (1962) has carried out a statistical analysis of type III dynamic spectra obtained between 180 and 9 MHz. He finds an average exciter speed of approximately 0.4c at the higher frequencies and a systematic decrease to 0.18c at the lower frequencies. This implies a deceleration of the type III exciter over distances of only a few solar radii. However, as Malville noted, this result may not be due to exciter deceleration but rather to an inappropriate choice of the electron density model. Stewart (1965) has analyzed in detail the variation of radial exciter speed with height for some 50 type III bursts covering the frequency range from 210 to 7 MHz observed with the Dapto spectrograph. He concludes that over the range of heights from 1.5 to 3 $R_\odot$ above the photosphere, the exciter speed is constant with an average value of 0.33c.

The application of this technique becomes even less certain beyond 10 $R_\odot$ where little is known about either exciter speeds or the electron density gradient in the outer corona, except at distances of the orbit of the earth, 212 $R_\odot$, where in situ measurements of the solar wind have been obtained with space probes. Between 10 and 80 $R_\odot$, observations of radio source scintillations caused by density fluctuations in the corona (e.g. Erickson, 1964) give an estimate of the density shape of the corona. But this technique has not as yet provided

a reliable density gradient because the distribution of irregularities is not known sufficiently well.

Observations of type III bursts at frequencies below 5 MHz can provide the information required to determine exciter speed and the electron density gradient between 10 and 100 $R_{\odot}$. However these low frequency observations must be conducted by space vehicles operating above the ionosphere where only low angular resolution antennas such as the short dipole have been used. The source position, therefore, cannot be directly observed and one must again rely on the interpretation of dynamic spectra as discussed above. This type of approach has been used by a number of groups working with space data (Hartz, 1964; Slysh, 1967; Hartz, 1969; Alexander et al., 1969; Haddock and Graedel, 1970). In one of the experiments conducted by Slysh (1967b), the circumstances of a lunar occultation as well as the modulation of the antenna reception pattern by the spacecraft spin were utilized in an attempt to locate the position of a type III source. Except for this attempt at source location, all space observations have been interpreted with a model of exciter speed or density gradient. In one variation (Hartz, 1969 ; Alexander et al., 1969) an energy density argument is invoked between the streamer (along which the emission is assumed to occur) and the ambient solar wind.

This requires the use of a solar wind model.

II. THE TYPE III STORM DRIFT RATE ANALYSIS

Part I of this series (Fainberg and Stone, 1970) presented the morphology of a storm of type III bursts observed in the 5 to 0.2 MHz frequency range by the RAE-I satellite. Such storms, composed of tens of thousands of drifting bursts, indicate the quasi-continuous production of type III events which can be observed for the entire period of rotation of the active region from the east to the west limb of the sun. When the same active region occurs again on the east limb a half rotation later, storm activity is again observed. This shows that the storm can in some cases persist for more than a complete rotation. The stability of the storm properties over at least a half solar rotation and the very large number of observed type III bursts provide an opportunity to investigate statistically a number of properties such as the exciter speeds.

As shown in Part I (Fainberg and Stone, 1970) the burst occurrence rate and apparent drift rates show a dependence on the heliographic longitude of the associated active region (McMath plage 9597). Both the occurrence and apparent drift rates are maximum near CMP, and minimum near the limb location of the active region.

For the present analysis, approximately 2500 drifting bursts were selected on the basis of a clear identification of their drift rate. Figure 1 and 2 show the distribution of these drift times per two-second drift interval for each storm day. In these figures, the histograms show the number of bursts used in the analysis and not the total number observed on that day. These data are grouped into twenty-four-hour periods for convenience in displaying the results. However, in the actual analysis the data were handled on a continuous time basis. For the present purposes only the data from the fixed frequency channels, 0.54, 0.70, 0.995, 1.31, 1.65 and 2.8 MHz were used because of the better time resolution. Eventually the analysis will be extended to the full range of the sweep receiver, 0.2 to 5.4 MHz, in order to extend our results from less than 10 $R_\odot$ to more than 60 $R_\odot$.

This apparent drift rate dependence on heliographic longitude can be explained in terms of the "light time" between the source and the observer. The observed drift rate depends not only on the time required for the exciter to travel between two plasma levels but also on the time difference for the radio emission to travel from the two plasma levels to the observer. The distances involved are so large that this time of flight correction may be quite important. For propagation in free space, a time of 23 seconds is required to travel a distance corresponding

to 10 $R_\odot$. When the type III events occur near the limb, the correction is smaller than when the emission occurs near central meridian.

The analysis proceeds on the basis of the geometry shown in Figure 3. An XYZ frame is chosen such that the XY plane is in the ecliptic, and the YZ plane contains the solar rotation axis. Let S denote the active region at colatitude ℓ. The burst observed at frequency f_i originates at P_i located radially above S at a distance r_i from the center of the sun. The same burst observed at a lower frequency f_j originates at P_j located a distance r_j along the same radial line. As the exciter moves radially outward, with velocity β ($\beta = v/c$), it excites radio emission of frequency f_i at P_i and of frequency f_j at P_j at an interval of time later of

$$T_{ji} = \frac{r_{ji}}{\beta c}$$

where $r_{ji} = r_j - r_i$, c is the velocity of light, and $\beta = v/c$ is the exciter speed in units of c. But the drift time t_{ji} observed at the earth is modified by the difference in transit times from P_i and P_j.

$$t_{ji} = \frac{r_{ji}}{\beta c} + \frac{R_j - R_i}{c}$$

Where R_j and R_i are the distances from P_j and P_i to the earth.

The remainder of the geometry is discussed in Appendix A. From this geometry, an expression for t_{ji} is calculated as a function of r_i, r_{ji}, β, t_s, and t. We can also include an additional term to this equation to take into account group delay in the path between source and observer.

But the observations of drift time for each burst between two frequencies f_i and f_j yields a value of t_{ji}^m, where the number of observed events may range into the thousands. With such large numbers of bursts available, it is possible to use a least squares analysis to derive the best values of r_{ji}, β, and t_s. This amounts to minimizing the function

$$\sum_m (t_{ji} - t_{ji}^m)^2$$

and the details are summarized in Appendix B.

RESULTS

The values of β, the exciter speed, obtained from this analysis are shown in Table I along with the frequencies between which the drift was determined and the number of bursts involved in the analysis. The values of distance listed in Table I were obtained from a previous analysis of dynamic spectra (Alexander et al., 1969). These values of distance for the plasma levels will be reexamined in Part III of this series, taking into account the results of the storm data analysis.

TABLE I

DETERMINATION OF EXCITER SPEED

Frequency Interval (MHz)	No. of Bursts Used in Analysis	Distance Between Plasma Levels, in $R_\odot$	$\beta = \frac{v}{c}$
2.8 -1.65	397	11 - 16	0.47
1.65 -1.31	1497	16 - 19	0.37
1.31 -0.995	847	14 - 24	0.35
0.995-0.700	250	24 - 30	0.31
			$\langle\beta\rangle = 0.38$
2.8 -1.31	272	11 - 19	0.43
2.8 -0.995	131	11 - 24	0.42
1.65 -0.995	614	16 - 24	0.36
1.31 -0.700	172	19 - 30	0.32
1.65 -0.700	128	16 - 30	0.28
			$\langle\beta\rangle = 0.36$

Table I shows exciter speeds derived from the data between the listed frequencies. The lower part of the table also shows the same information but it was computed independently for those bursts extending over the larger frequency intervals. This was done to check the consistency of the results given in the upper part of Table I. The simple average exciter speed between 2.8 and 0.7 MHz, which corresponds to a total distance of about 19 $R_\odot$, is 0.38c while the average, weighted according to the number of bursts used in the analysis, is nearly the same (0.37c). Table I also suggests a systematic deceleration with radial distance but such a conclusion is unfounded at this point. Note that the

values which deviate most from the average are based on a smaller number, less than one half, of the bursts available between 1.65 - 0.995 MHz. In the analysis, all drift rate measurements within 3.5 standard deviations were retained. Within these limits, which included virtually all data points, there is however a considerable spread of drift rates. This suggests the need for a large sample before a convergence to a mean value is obtained. To estimate the sample size required for convergence, the drift rate data between 1.65 and 1.31 MHz (for which 1500 bursts are available) were reexamined by conducting the same least squares analysis with a sample of fewer bursts. A value of $\beta \sim 0.37$ was maintained until the sample size was less than 300 bursts. For fewer data points the derived value of β began to fluctuate by more than 20% and below a few hundred bursts became meaningless. This analysis suggests that the 0.995 - 0.700 interval data in Table I, for which only 250 entries were used, is less reliable.

In arriving at the results in Table I, a number of assumptions have been made. First, the influence of the dispersive properties of the medium on propagation time has been neglected. The excess time of signal transmission through the corona has been considered, for example, by Jaeger and Westfold (1950), and Wild et al., (1959). Such considerations show that if the radiation occurs at the plasma

frequency in the ambient corona, then the major contribution to the excess time occurs in a small region near the source where the index of refraction of the medium is considerably less than unity. However, as indicated earlier in this paper, type III bursts appear to be observed when they occur in active region streamers having an average density enhancement above the ambient corona. A comprehensive review of streamer structure was given by Newkirk (1967). The existence of a density enhancement seems to be confirmed for the low frequency range by investigators attempting to derive coronal properties from type III dynamic spectra (Alexander et al., 1969; Hartz, 1969). The fact that type III bursts can be observed at the limb position of the associated active region also confirms this. If the emission originates within a streamer and then escapes to the ambient corona of lower density, the group delay time correction can be expected to be much less than that which would exist if the emission occured in the ambient corona. It is also likely that because of density inhomogeneities in the streamer, the emission is able to escape over a wide range of angles (Morimoto 1964).

To investigate this question further, noting that the group delay time would be most important for larger heliographic longitudes, we recomputed the least squares program with the analysis confined to data corresponding to heliographic longitudes within 45^{o} of CMP; we obtained essentially the same results as

shown in Table I.

We have also assumed that the average exciter speed and streamer properties remain constant during the period of observation, i.e., a half solar rotation for the present analysis. The validity of this assumption was verified by dividing the data into heliographic longitude sectors and analyzing them separately. This assumption is also supported by the fact that no large scale changes of the active region were observed during this period. For example, the lists of solar flares contained in the montly "Solar-Geophysical Data" issued by ESSA in Boulder, Colorado contain no flares larger than 1N. In addition, the 9.1 cm and 21 cm radio maps (from Stanford University and the University of Sydney, respectively) show a relatively stable structure and in fact, closely resemble the maps for the same active region one solar rotation earlier.

A third assumption of the analysis is that the exciter travels radially outward on the average. This is the only reasonable guess in view of the present lack of knowledge about exciter paths. However, there is some evidence that solar magnetic fields swept out from the sun in comparable latitude regions return to the ecliptic plane by 1 A.U. (Wilcox and Ness, 1967). If the exciters are influenced by these fields, then a nonradial path at large distances from the sun is indicated. This should not greatly influence the present results which apply to the first 20 percent of the path to the earth.

DISCUSSION

The values of β shown in Table I are average drift rates between the frequency intervals shown; the spread of drift rate about this average value can be seen in Figures 1 and 2. In these figures the dots indicate the best fit as derived from the least squares analysis. The spread of drift rates can be interpreted as either a variation of electron density gradient through which the exciters move or a real spread of exciter speeds or both. If we interpret the spread as due to exciter speed variations, we find that $0.2 \lesssim \beta \lesssim 0.6$. However, for reasons which will be examined in detail in Part III of this series, we believe that the spread in drift rates is due primarily to streamer density inhomogeneities through which individual exciters travel.

The techniques discussed in this paper will be extended with additional RAE-I data to obtain a larger statistical sample and a wider frequency range. But we also suggest that it might be possible, with adequate time resolution, to apply the same technique to the type III component of decametric continuum.

One of the advantages of dealing with this storm event statistically is that probably all of the type III events come from the same active region, providing therefore some degree of uniformity. We are investigating other type III storms in order to determine if the average exciter speed obtained is the same

for all such storms. Another question to be considered is whether the average exciter speed derived for storm events is also typical of isolated type III bursts. This appears to be the case based on a preliminary comparison between the storm type III drift rates and those of isolated (nonstorm) type III's where we could estimate the associated flare longitude.

CONCLUSION

We believe that the exciter speeds derived in this paper represent the first reliable determination of this quantity in the coronal height range between 10 and 30 $R_\odot$. Within the limitations discussed above, the average exciter speed appears to be constant at approximately 0.37c. If the exciter packet were composed of monoenergetic electrons, the speed of 0.37c would correspond to electrons with kinetic energy of 40 keV.

Direct observations of the type III source (Wild 1960, Kundu et al., 1970) for heights within a few solar radii of the chromosphere yield exciter speeds of about 0.4c. The analysis of dynamic spectra by Stewart (1963) between 1.5 and 3 $R_\odot$ yielded exciter speeds of 0.33c. Combined with the present result of 0.37c for $10 \lesssim \frac{R}{R_\odot} \lesssim 30$, it would appear that over a height range of 30 $R_\odot$ the exciter undergoes little if any deceleration. Moreover, space probes making in situ particle measurements beyond the magnetosphere detect the presence of streams of

electrons, presumably of solar origin, with energies of 40 keV. (Van Allen and Krimigis, 1965; Lin and Anderson, 1967, Lin, 1969). It is suggested by these authors that electrons produced somewhere in the vicinity of the sun fill the magnetic field lines originating at the injection point near the sun. The electrons are channeled along these field lines out through the interplanetary medium.

The present determination of exciter speed for the mid range in the interplanetary medium establishes a link between processes close to the sun and the detection of energetic electrons of solar origin near the earth. A preliminary study indicates a correlation between many type III bursts observed by RAE-I and the delayed occurrence of enhanced fluxes of $\lesssim$ 40 keV electronsof solar origin measured by Lin and Anderson (1967). Clearly this analysis will be of great importance in the investigation of both the transport and dispersion of energetic particles in the interplanetary plasma. At this point it seems appropriate to assert only that the exciters appear to be packets of superthermal electrons of average energy $\lesssim$ 40 keV, which are able to propagate over distances of the order of 1 A.U. with little deceleration. The dispersion of the electrons in space or energy remains an additional problem to be discussed later. Such information may be inferred from a combination of the type III

burst profile data and the energy spectrum of the solar electrons detected beyond the magnetosphere. Part III of this series will continue the analysis to obtain specific information on properties of the streamer such as its average electron density and the scale of density inhomogeneities. This analysis also leads to an estimate of the bulk solar wind speed in the 10 to 30 $R_{\odot}$ distance range.

REFERENCES

Alexander, J.K., Malitson, H.H., and Stone, R.G.: 1969, Solar Phys. 8, 388-397.

Allen, C.W.: 1947, Mon. Not. Roy. Astron. Soc. 107, 426.

Elgaroy, O., and Rodberg, H.: 1963, Nature 199 268.

Erickson, W.C.: 1964, Astrophys. J. 139, 1290-1311.

Fainberg, J., and Stone, R.G.: 1970, submitted to Solar Phys.

Haddock, F.T. and Graedel, T.E.: 1970, Astrophys. J. 160 293-300.

Hartz, T.R.: 1964 Ann. d'Astrophys. 27, 831-837.

Hartz, T.R.: 1969, Planet. Space Sci., 17, 267-287.

Hughes, M.P. and Harkness, R.L.: 1963, Astrophys. J. 138 239.

Jaeger, J.C. and Westfold, K.C.: 1950, Austral. J. Sci. Res. A3, 376-386.

Kuckes, A.F. and Sudan, R.N.: 1969, Nature 223, 1048-1049.

Kundu, M., 1965, Solar Radio Astronomy, Interscience, New York.

Kundu, M.: 1970, Private communication.

Lin, R.P. and Anderson, K.A.: 1967, Solar Phys. 1 446-464.

Lin, R.P.: 1969, Private communication.

Malville, J.M.: 1962, Astrophys. J. 136 266-275.

Morimoto, M.: 1964, Publ. Astron. Soc. Japan 16, 163.

Newkirk, G., Jr.: 1961, Astrophys. J. 133, 983-1013.

Newkirk, G., Jr.: 1967, Ann. Rev. Astron. Astrophys. 5, 213-266.

Stewart, R.T.: 1965, Austral. J. Phys. 18, 67-76.

Slysh, V.I.: 1967a, Astron. Zh. 44, 487-489 (Soviet Astron.-A.J. 11, 389-391).

Slysh, V.I.: 1967b, Kosm. Issled. 5, 867-910.

Takakura, T.: 1967, Solar Phys. 1, 304-353.

Van Allen, J.A. and Krimigis, S.M.: 1965, J. Geophys. Res. 70 5737-5751.

Wilcox, J.M. and Ness, N.F.: 1967, Solar Phys. 1, 437-445.

Wild, J.P.: 1950, Austral. J. Sci. Res. A3, 541-557.

Wild, J.P., Roberts, J.A., and Murray, J.D.: 1954, Nature 173 532.

Wild, J.P., Sheridan, K.V., and Neylan, A.A.: 1959, Austral. J. Phys. 12, 369-398.

Wild, J.P., Smerd, S.F., and Weiss, A.A.: 1963, Ann. Rev. Astron. Astrophys. 1, 291-366.

APPENDIX A

The drift time t_{ji} of the burst peak from frequency f_i to frequency f_i as observed at the earth is modified by the difference in transit times of the emissions from P_i and P_j (figure 3). We have

$$t_{ji} = \frac{r_{ji}}{c\beta} + \frac{R_j - R_i}{c} \tag{A1}$$

where

c = velocity of light

β = velocity of exciter relative to c

$R_j = \overline{P_j\ E}$

$R_i = \overline{P_i\ E}$

$r_{ji} = \overline{P_i\ P_j} = r_j - r_i$

The position of the earth is at $E = (X_E, Y_E, O)$

where

$$\begin{aligned} X_E &= R_E \cos(\omega_E t + \phi_E) \\ Y_E &= R_E \sin(\omega_E t + \phi_E) \end{aligned} \tag{A2}$$

Here R_E is the earth-sun distance and ω_E is the earth's orbital angular velocity which are both nearly constant over

the period of the analysis. ϕ_E is the angle

$\lambda - \Omega = 1.2516$ rad. for t = 0 chosen as

0 UT, August 20, 1968

λ = geocentric longitude

Ω = longitude of ascending node

Also

$$P_i = (X_i, Y_i, Z_i) \tag{A3}$$

where

$$\begin{aligned} X_i &= r_i \sin \ell \cos [\omega_s (t - t_s)] \\ Y_i &= r_i \sin \ell \cos \alpha \sin [\omega_s (t - t_s)] + r_i \cos \ell \sin \alpha \\ Z_i &= r_i \sin \ell \sin \alpha \sin [\omega_s (t - t_s)] + r_i \cos \ell \cos \alpha \end{aligned} \tag{A4}$$

$\alpha = 7^o\ 15'$ - inclination of solar axis to ecliptic pole

ω_s = angular rotation of the sun at colatitude $\ell = 0.0103$ rad. per hr.

t_s = constant determined from the analysis which is related to the time of maximum drift rate (CMP of radio region); $t_s + 123.4^h$ is the time in hours after 0 UT August 20, 1968 of best fit for CMP of radio region

ℓ = colatitude of source (taken as 108^o from optical data)

APPENDIX B

We have then the expression for the drift time from A1 - A4 of

$$t_{ji} = f\,(r_i, r_{ji}, \beta, t_s, t) \qquad \text{(B1)}$$

as a function of the high frequency level r_i, the level separation r_{ji}, the exciter velocity β, the reference time t_s of maximum drift rate, and the time t. The measurement of the drift time of each burst between frequency f_i and frequency f_j yields t_{ji}^m where m ranges over the number of bursts available (in thousands for several frequencies)

In the range of interest, $r_i < 40\ R_\odot$, t_{ji} is not a sufficiently sensitive function of r_i for the derivation of r_i by the least squares procedure; a reasonable value of r_i was chosen for this quantity and the least squares procedure was used to derive best values of r_{ji}, β, and t_s. Later a self consistent method based on the values of r_{ji} obtained was used to choose values of r_i.

For the least square procedure we require

$$\sum_m (t_{ji} - t_{ji}^m)^2 = \text{minimum} \qquad \text{(B2)}$$

where m ranges over all the measured bursts.

We write $t_{ji} = f\,(r_i,\ r'_{ji} + \delta r_{ji},\ \beta' + \delta\beta,\ ts' + \delta ts, t)$ (B3)

when the prime variables are guessed values

and the δ terms are correction terms to be

calculated from the analysis

Necessary conditions for equation (B2) are:

$$\frac{\partial}{\partial r_{ji}} \sum_m (t_{ji} - t_{ji}^m)^2 = 0$$

$$\frac{\partial}{\partial \beta} \sum_m (t_{ji} - t_{ji}^m)^2 = 0 \qquad \text{(B4)}$$

$$\frac{\partial}{\partial t_s} \sum_m (t_{ji} - t_{ji}^m)^2 = 0$$

Keeping the first terms only in the Taylor expansion of t_{ji} we obtain a set of 3 linear equations:

$$\delta r_{ji} \sum_m \left(\frac{\partial t_{ji}}{\partial r_{ji}}\right)^2 + \delta\beta \sum_m \left(\frac{\partial t_{ji}}{\partial \beta}\,\frac{\partial t_{ji}}{\partial r_{ji}}\right) + \delta t_s \sum_m \left(\frac{\partial t_{ji}}{\partial t_s}\,\frac{\partial t_{ji}}{\partial r_{ji}}\right) =$$

$$\sum_m \left(t_{ji}^m - t_{ji}\right) \frac{\partial t_{ji}}{\partial r_{ji}}$$

$$\delta r_{ji} \sum_m \left(\frac{\partial t_{ji}}{\partial r_{ji}} \frac{\partial t_{ji}}{\partial \beta} \right) + \delta\beta \sum_m \left(\frac{\partial t_{ji}}{\partial \beta} \right)^2 + \delta t_s \sum_m \left(\frac{\partial t_{ji}}{\partial t_s} \frac{\partial t_{ji}}{\partial \beta} \right) =$$

$$\sum_m \left(t_{ji}^m - t_{ji} \right) \frac{\partial t_{ji}}{\partial \beta}$$

(B5)

$$\delta r_{ji} \sum_m \left(\frac{\partial t_{ji}}{\partial r_{ji}} \frac{\partial t_{ji}}{\partial t_s} \right) + \delta\beta \sum_m \left(\frac{\partial t_{ji}}{\partial \beta} \frac{\partial t_{ji}}{\partial t_s} \right) + \delta t_s \sum_m \left(\frac{\partial t_{ji}}{\partial t_s} \right)^2 =$$

$$\sum_m \left(t_{ji}^m - t_{ji} \right) \frac{\partial t_{ji}}{\partial t_s}$$

where t_{ji}, and its derivatives are evaluated at the initial values.

The solution of equations (B5) is a set of correction terms δr_{ji}, $\delta\beta$, δt_s which are added to the first guess and the procedure of (B3) to (B5) repeated to derive a second set of corrections $\delta r''_{ji}$, $\delta\beta''$, $\delta t''_s$. After 3 or 4 times around this loop the corrections become insignificant and a set of values are obtained for r_{ji}, β, and t_s which do not depend on the original choices. These values then represent the best fit of the model to the data for bursts drifting from frequency f_i to frequency f_j. The computer time necessary to solve (B5) with the summation extending over a thousands of bursts and the computer evaluating all the partial derivations is of the order of a minute. This procedure has been followed for data for all of the possible pairs of the six frequencies used in this analysis.

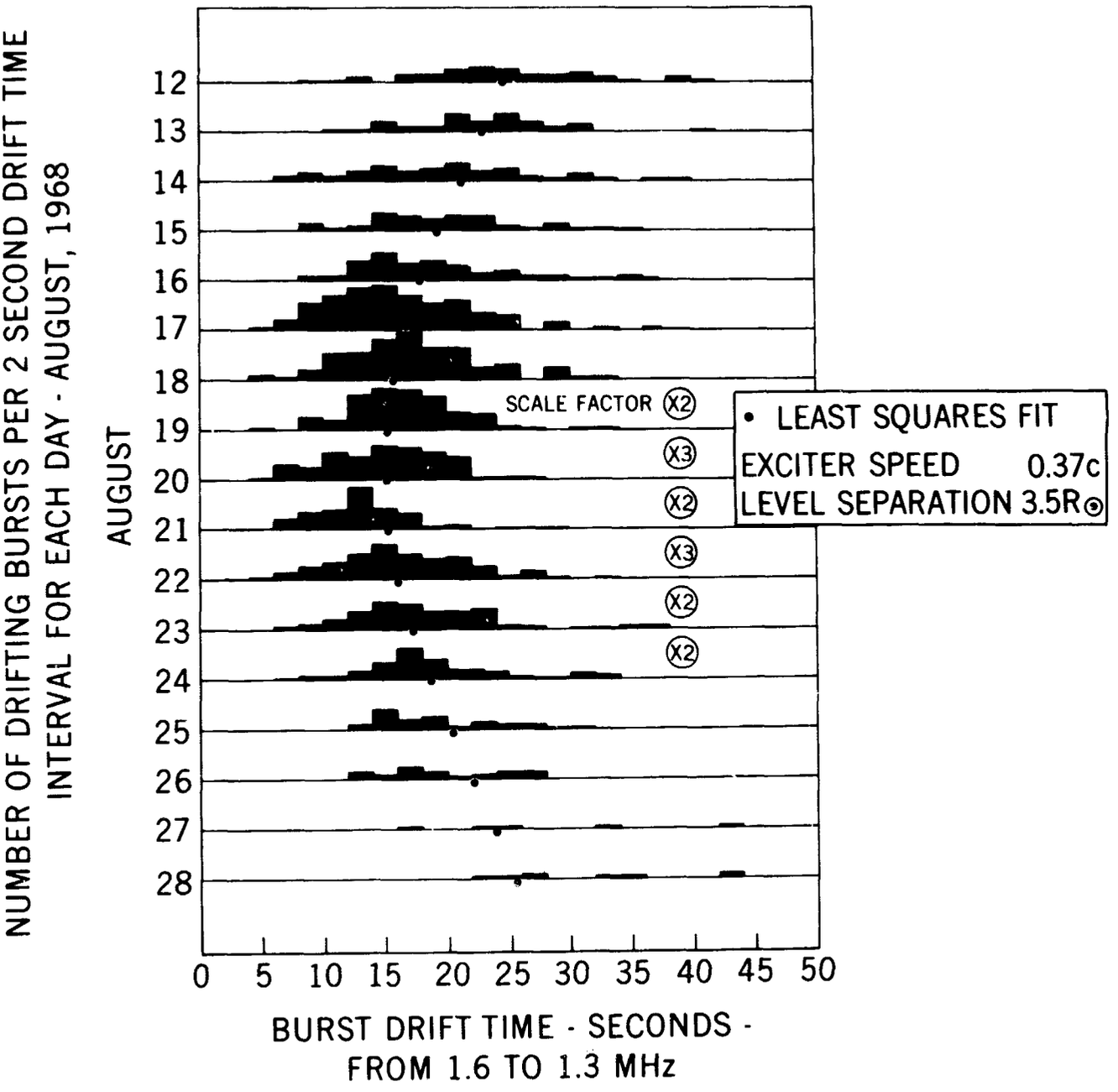

Figure 1 - Histograms of the number of bursts per two-second drift time interval vs. drift time for twenty-four-hour groups of bursts drifting from 1.6 to 1.3 MHz. The circled figures are vertical scale factors relative to 1 for active days. The dots are the drift times yielded by the model at the midpoint of each day for the least squares fit of the model to these data. For these data the least squares analysis yielded $\beta = 0.37C$ and level separation = 3.5 $R_{\odot}$. The number of bursts used was 1497.

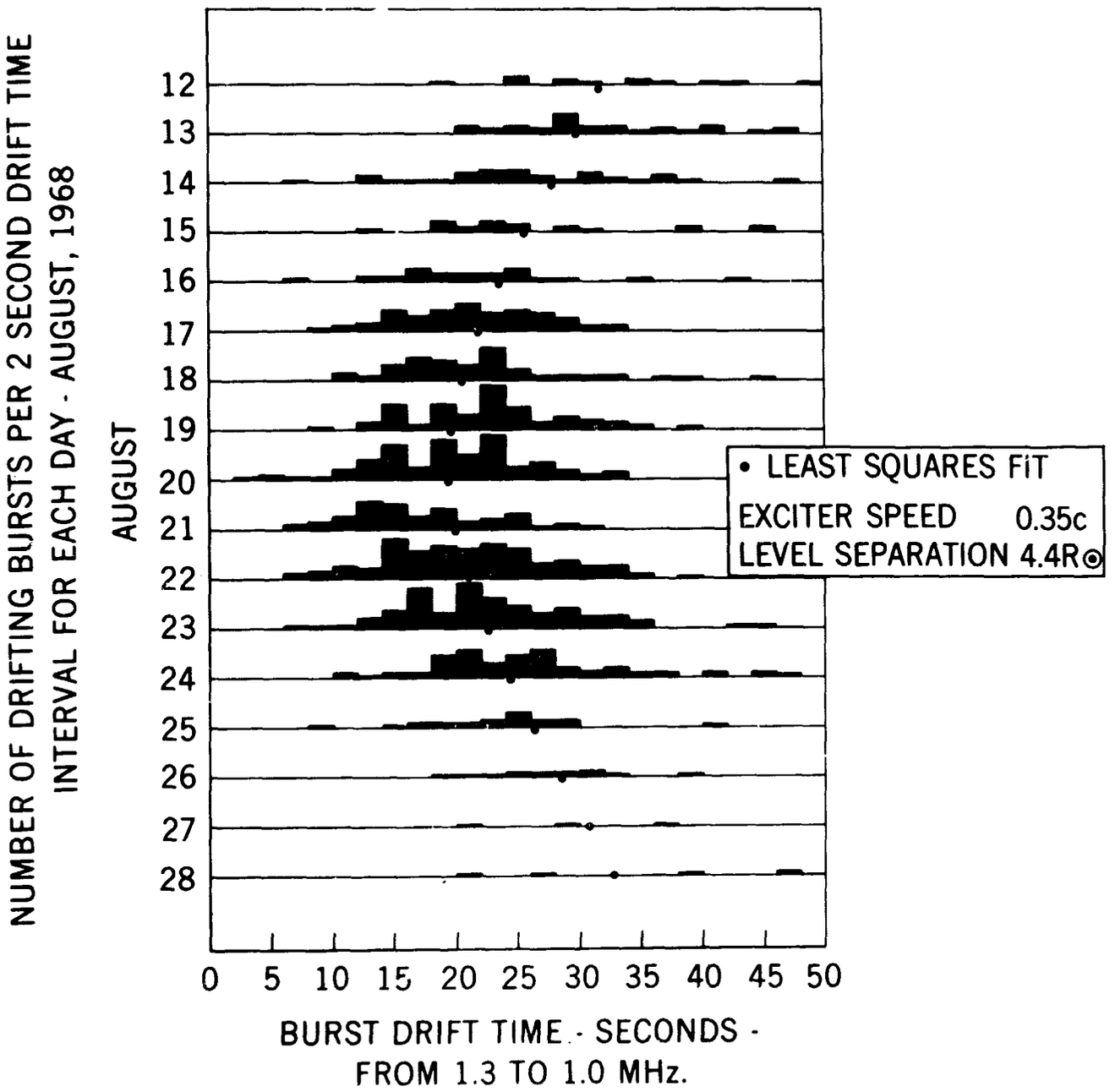

Figure 2 - Same type of plot as Figure 1 but for bursts drifting from 1.3 to 1.0 MHz. For these data the least squares fit yielded $\beta = 0.35C$ and level separation = 4.4 $R_\odot$. The total number of bursts used was 847.

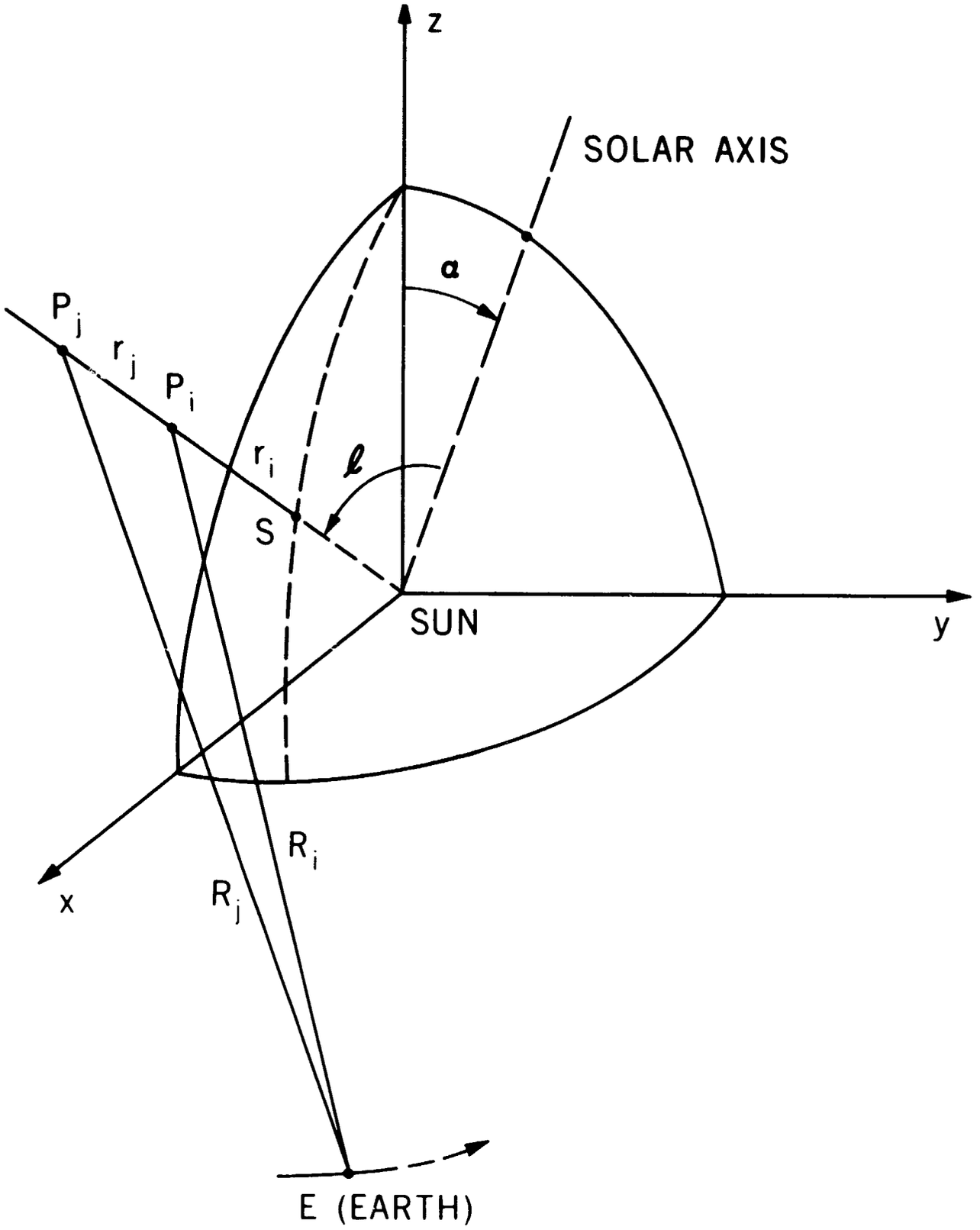

Figure 3 - Geometry of model. The center of the burst region at frequency F_j is found to lie radially above the center of the burst region at frequency F_i. The observed burst drift time reflects the exciter travel time from $\underline{P_i}$ to $\underline{P_i}$ as well as the difference in E.M. wave prapagation time along R_i and R_j.